OCEANOLOGY, English Translation, VOL. 34, NO. 2, OCTOBER 1994
Russian Edition: MARCH – APRIL 1994

TS-analysis of the Black Sea waters

O. I. Mamayev, V. S. Arkhipkin, and V. S. Tuzhilkin
M. V. Lomonosov Moscow State University

Abstract. A TS-analysis was performed for the entire water column, for August and February separately. The following displays are presented: (a) TS-scatter diagrams for the entire water column; (b) three-dimensional volumetric TS-diagrams and quantitative TS-diagrams showing volume, enthalpy and salt content for each TS-class; (c) averaged long-term "stations" showing potential temperature, vertical stability, and Väisälä-Brunt frequency. For all the diagrams, the water masses are distinguished, namely the near-surface water (NSW), the cold intermediate layer (CIL), and the deep water. The NSW and CIL vary seasonally, while the deep water remains unaltered. The total volume and the salt content of NSW+CIL remain constant throughout the year, the only change being their redistribution between these two layers. Between August and February, the surface layer gives up its heat content to the CIL and to the atmosphere. The TS-analysis presented is based on a modern hydrological data set.

1. Introduction

The Black Sea hydrological structure has many anomalous features that distinguish it from the World Ocean's typical water mass structure. The following features are especially remarkable:

(1) strong seasonal variability of the upper layer, from the sea surface to the lower boundary of the cold intermediate layer (CIL);

(2) a permanent CIL, well developed in summer and nearly unnoticed in winter when the CIL is almost merged with the surface layer which is very cold in winter and very warm in summer;

(3) long-term stability of the hydrological structure of the bulk of the sea's water column, from 75–100 m to more than 2000 m, down to the bottom;

(4) monotonic, gradual increase of the temperature of this water column with depth, accompanied with a salinity increase with depth; this gradual temperature increase is a unique feature of the Black Sea, which never is observed to such an extent and so deep in the World Ocean.

Detailed characteristics of these features (long known in a general sense) may be obtained with TS-analysis, a powerful tool for studying oceanographic structure. The example of the Black Sea illustrates very vividly the efficacy of TS-analysis.

In this work we present and discuss:

(a) TS-scatter diagrams for the entire water column, for August and February, because these two months are the most conspicuous examples of the extremes of the summer and winter conditions of the Black Sea waters during their seasonal evolution;

(b) volumetric characteristics, namely three-dimensional volumetric TS-diagrams as well as quantitative statistical diagrams (for each TS-cell) for volume, enthalpy, and salt content, for August and February;

(c) long-term averaged "mean" stations for the entire Black Sea, for August and February, which allow the anomalies (especially in the upper layers) to be studied.

The TS-analysis of the Black Sea waters presented below is based on the most complete up-to-date hydrological data set briefly described in Section 5.

2. *TS*-Scatter Diagrams

A TS-scatter diagram is a set of TS-points corresponding, as a rule, to the standard levels, for a large number of oceanographic stations occupying an area in question, plotted in the same TS-coordinates, on the same diagram. These diagrams are well known in oceanography; however before the computer era they were a rarity because the manual plotting of data points was too laborious and conducive to numerous errors. The first computer-generated TS-diagrams have shown their high efficacy in water mass studies. We could refer to the TS-scatter diagram for 158°W constructed by Wyrtki and Kilonsky (see *Mamayev* [1987], Figure 6.1) as a good example. In this diagram, the South Pacific water masses are distinguished very clearly. The more data points are present in the diagram, the more distinct are the water masses. This example is not unique in the modern literature.

The TS-scatter diagrams for the Black Sea may be found in a work of *Ozsoy et al.* [1991], although they are constructed for a limited number of stations of a

Copyright 95 by the American Geophysical Union.
0001–4370/95/3402–0003$18.00/1

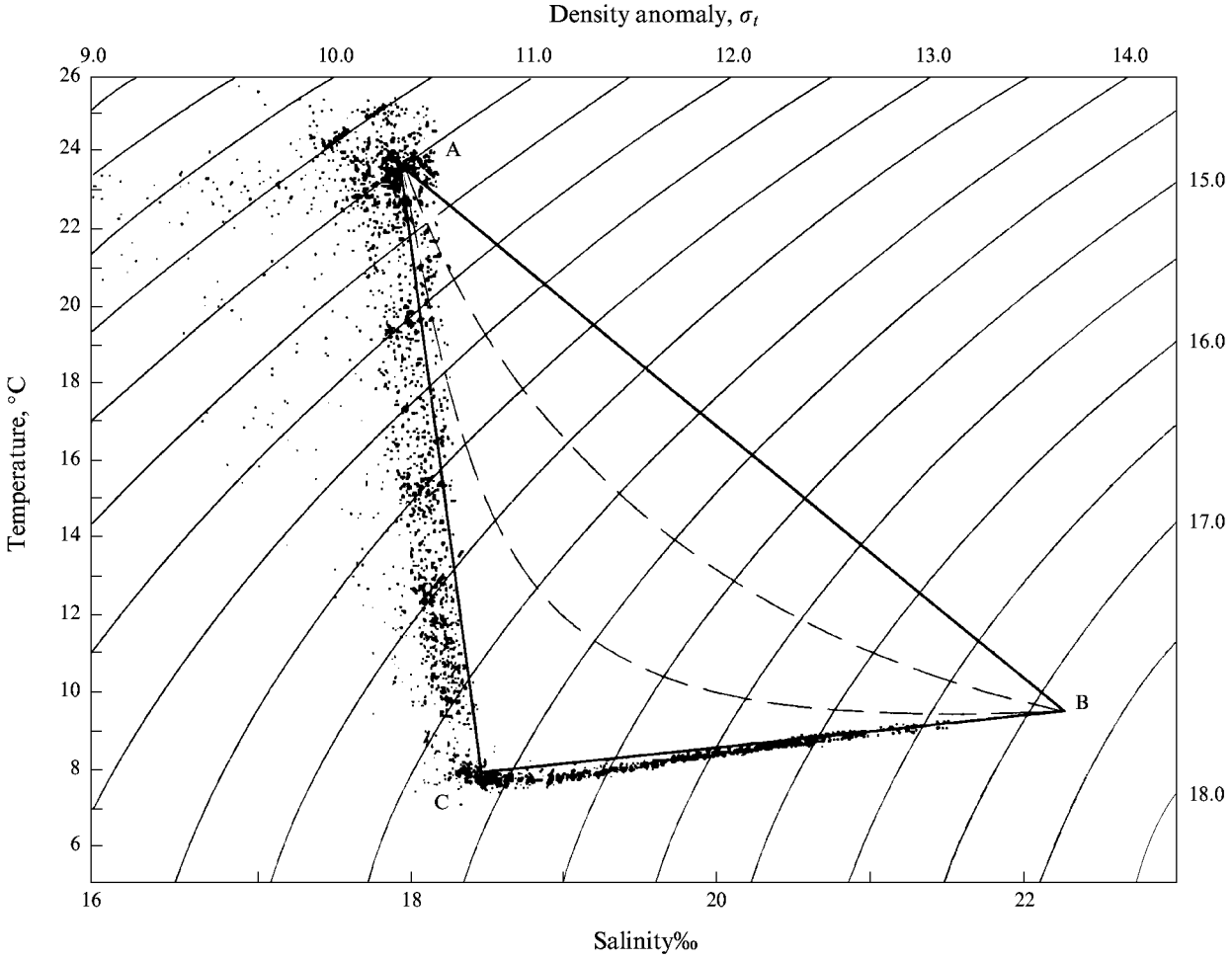

Figure 1. The TS-scatter diagram of the Black Sea waters for August. Dashed lines show the TS-curves produced, in accordance with the analytic theory of TS-curves, by the symmetric mixing of the intermediate water mass C with the surface water mass A and the deep water mass B (see text). Solid lines show the mixing triangle.

single summertime survey in the southern part of the sea, and therefore they cannot characterize either the seasonal variability of the upper layers of the Black Sea, or its long-term conditions. These aspects are presented below.

Figures 1 and 2 show TS-scatter diagrams for the Black Sea for the summer (August) and winter (February), constructed from hydrological data in the cell centers of a regular grid, $21'$ latitude by $28'$ longitude, covering the entire sea, at each standard level (up to 23 levels from 0 to 2000 m) (see Section 5). The total number of data points is 5141.

The freshened coastal waters with $S < 16‰$ (a narrow zone in the shallow, near-shore, northwestern part of the sea) were excluded from the analysis; hence the TS-scatter diagrams represent the deep waters that comprise 99.9% of the total volume of the sea.

Analysis of the diagrams allows us to come to the several conclusions about the thermohaline water mass structure and its seasonal variability. These diagrams make it possible to take another look at some well-established facts. The conclusions drawn from the scatter diagrams are the following:

The summertime 0–50 m layer (the AC-band in Figure 1) displays stratification classified as "unconditional stability": $dT/dz < 0$, $dS/dz > 0$, $E_\theta > 0$, $E_S > 0$ (the definitions of stability parameters E_θ, E_S, and E are given in the Comment to Table 1). This stratification is obliterated during fall/winter mixing (the vertical wintertime circulation) due to a large heat loss to the atmosphere, so that the summer cluster (the densest subset of points) of surface waters centered at $T \simeq 23°C$, $S \simeq 18.25°C$ (Figure 1) is changed into the winter cluster centered at $T \simeq 7°C$, $S \simeq 18.5°C$ (Fig-

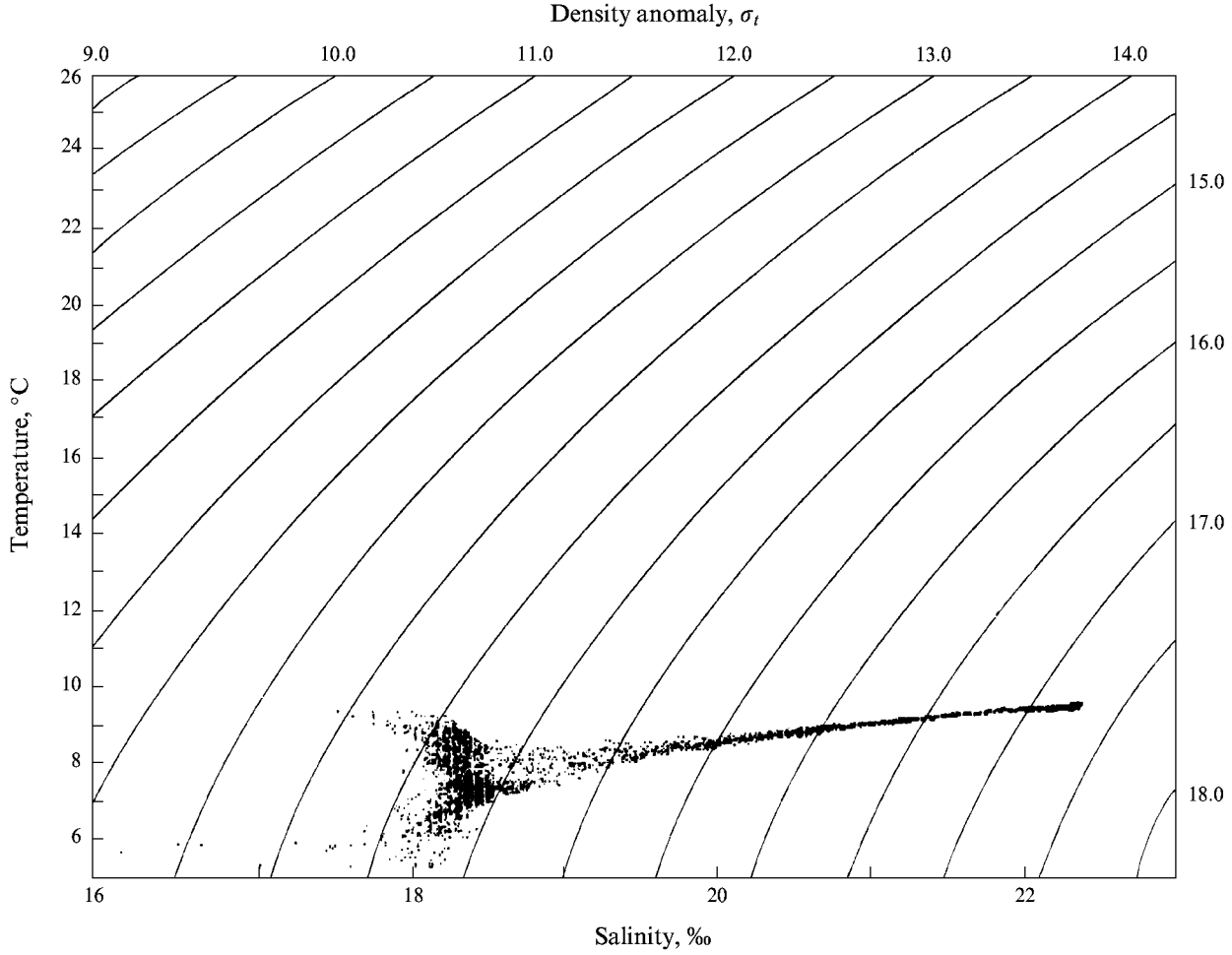

Figure 2. The TS-scatter diagram of the Black Sea waters for February. The scales are the same as in Figure 1.

ure 2). This is a future core of the cold intermediate layer. During the fall/winter transformation the temperature decreases by $\sim 16°C$, while the salinity of the core of the winter cluster is slightly higher than that of the summer cluster, about $0.25‰$.

As noted earlier, from 75–100 m to $\sim$2000 m, the temperature and salinity increase with depth, which is not typical of the bulk of the abyssal World Ocean in the low-to-temperate latitudes. The TS-scatter diagrams display this feature against isopycnals allowing us to estimate the stability. The stratification has the form: $d(T,S)/dz > 0, E_\theta < 0, E_S > 0, E > 0$. The temperature stability is negative, although the positive salinity stratification prevails; the density ratio is very small and negative (Tables 1 and 2). These conclusions imply the probable existence of weak mixing in the deep Black Sea, of the double-diffusion type, with different rates for salinity and temperature (see *Mamayev* [1987], Figure 4.6). This aspect is discussed in more detail in a recent paper [*Ozsoy et al.*, 1991].

The warm surface layer of the Black Sea is thus very "vulnerable" and is obliterated quickly during fall and winter. This layer could be referred to as a "warm pool," the term usually applied to the warmest waters of the World Ocean, the near-equatorial waters of the Indonesian seas and east of them.

The TS-diagram for August is clearly L-shaped. In the framework of the analytic theory of TS-curves by Stockman, this diagram may be considered a manifestation of interaction of three water masses, the surface waters mass A, the intermediate water mass B, and the deep water mass C. In this case the L-shape suggests very weak mixing of the water masses A and B via the intermediate water mass B, or even the absence of interaction between them, otherwise the TS-curve within the mixing triangle ABC would be of a more rounded form like, for example, the two dashed curves in Figure 1. Such shapes are typical, for instance, of the TS-curves in the northeastern Pacific, where a rounded extreme belongs to the subarctic intermediate

Table 1. The average oceanographic station of the Black Sea for August

Pressure P, dbar	T,° C	S, ‰	θ,° C	$10^8 \cdot E$	$10^8 \cdot E_\theta$	$10^8 \cdot E_S$	$-E_\theta/E_S$	NB
0	23.817	17.474	23.817					
5	23.131	17.668	23.130	7085.5	4295.0	2790.5	−1.54	15.17
10	22.179	17.849	22.177	12087.4	9754.2	2333.2	−4.18	19.81
15	19.289	17.981	19.287	15656.3	13752.2	1904.0	−7.22	22.54
20	16.138	18.103	16.135	13561.3	12068.0	1493.3	−8.08	20.97
25	13.177	18.179	13.174	10401.2	9165.5	1235.7	−7.42	18.36
30	10.656	18.266	10.653	5705.6	4525.8	1179.8	−3.84	13.59
50	7.797	18.534	7.793	2246.2	781.0	1465.2	−0.53	8.53
75	7.740	19.149	7.734	2008.1	−53.6	2061.7	0.03	8.06
100	8.047	19.873	8.039	1754.6	−123.7	1878.4	0.07	7.53
125	8.283	20.371	8.273	1319.2	−99.9	1419.1	0.07	6.53
150	8.470	20.797	8.458	934.8	−66.7	1001.5	0.07	5.49
200	8.647	21.251	8.630	505.2	−32.7	537.9	0.06	4.04
250	8.736	21.499	8.714	309.5	−17.5	327.0	0.05	3.16
300	8.791	21.678	8.765	204.5	−9.8	214.2	0.05	2.57
400	8.847	21.881	8.811	131.3	−4.0	135.2	0.03	2.06
500	8.868	22.033	8.823	90.8	−1.1	91.9	0.01	1.71
600	8.882	22.122	8.827	53.9	−0.4	54.4	0.01	1.32
800	8.904	22.229	8.830	30.7	−0.4	31.2	0.01	0.99
1000	8.934	22.287	8.840	14.5	−0.8	15.3	0.05	0.68
1200	8.966	22.310	8.851	6.8	−0.1	6.9	0.02	0.47
1500	8.987	22.330	8.840	3.3	0.8	2.5	−0.31	0.33
2000	9.013	22.331	8.810	3.2	1.4	1.8	−0.81	0.32

θ – potential temperature; E – stability parameter ($E = E_\theta + E_S$, dbar^{-1}); E_θ – thermal stability, E_S – salinity stability; ($E_\theta = \alpha d\theta/dp$, $E_S = \beta dS/dp$); α – thermal expansion coefficient; β – salinity contraction coefficient; $-E_\theta/E_S$ – density ratio; NB – Väisälä-Brunt frequency (cycle/hour).

water mass. Further examples of analogous TS-curves may be found, e.g., in the work of *Mamayev* [1987].

Thus, the L-shaped TS-curves suggest that the deep water mass B is mixed only with the intermediate water mass C, which is reinforced by the TS-relationship for February. This fact was noted earlier [*Mamayev*, 1986]: the surface water mass A is too short-lived to participate in the gradual process of mixing with water masses B and C.

3. Volumetric TS-Analysis

This volumetric TS-analysis of the Black Sea waters is not the first one: it was done earlier by *Glazkov* [1970], who analyzed the water mass distribution from data of 145 deep (down to the bottom), summertime (June to September) oceanographic stations. His results still do not allow us to estimate the seasonal changes of the upper near-surface layer and the cold intermediate layer, although the summer conditions and thermohaline peculiarities of the deep layer have been described by Glazkov quite reliably. Gertman (in *Chernoye Morye* [1991] has given the volumetric TS-diagrams for the winter and summer seasons (Figure 2.23); however the volume distributions are shown with isolines (the relief isopleths), not with the numbers showing the volume in each TS-class, thus not allowing the seasonal water movements between classes to be evaluated. Additionally, in his diagrams the peak that is typical of the deep waters cannot be discerned. However, Gertman shows the separate distribution of the deep waters (for $S > 20$‰) and has calculated the $T(S)$ and $S(T)$ regressions for these waters. Lastly, his work contains useful tables of characteristics (volume, heat/salt content, mean temperature and salinity) for the entire Black Sea, for various seasons and for individual water masses (the upper water mass, the cold intermediate layer, the intermediate water mass, and the deep water mass, distinguished by their salinity). He used 0.2‰ × 1°C subdivisions for the entire sea, with 0.2‰ × 2°C subdivisions for the deep waters.

In this work, the TS-analysis was performed using a regular grid described in Sections 2 and 5. The entire water column was divided by linear interpolation into 5-m layers, which were used for integration using 0.2‰ × 0.51°C TS-classes, with subsequent multiplication of station data by the area of trapezoid or its part. The results of the volumetric analysis are presented below for the summer (August) and winter (February) separately, as follows:

Table 2. The average oceanographic station of the Black Sea for February. The notations are as in Table 1

Pressure P, dbar	T,°C	S, ‰	θ,°C	$10^8 \cdot E$	$10^8 \cdot E_\theta$	$10^8 \cdot E_S$	$-E_\theta/E_S$	NB
0	6.987	18.009	6.987					
5	6.986	18.121	6.986	1339.2	−36.6	1375.8	0.03	6.58
10	7.026	18.187	7.025	916.6	−103.3	1019.8	0.10	5.45
15	7.094	18.253	7.093	647.9	−61.6	709.6	0.09	4.58
20	7.090	18.279	7.089	482.9	−141.6	624.5	0.23	3.35
25	7.240	18.334	7.238	579.0	−179.5	758.5	0.24	4.33
30	7.271	18.377	7.269	719.6	−59.2	778.8	0.08	4.83
50	7.386	18.609	7.383	1253.6	−107.6	1361.2	0.08	6.37
75	7.770	19.201	7.764	1758.0	−152.2	1910.2	0.08	7.54
100	8.086	19.849	8.078	1719.6	−119.3	1838.9	0.06	7.45
125	8.292	20.397	8.282	1375.3	−89.8	1465.1	0.06	6.67
150	8.466	20.803	8.454	920.3	−64.7	985.0	0.07	5.45
200	8.653	21.275	8.636	514.8	−34.1	549.0	0.06	4.08
250	8.743	21.570	8.721	306.5	−18.1	325.6	0.06	3.14
300	8.801	21.699	8.775	205.9	−10.0	215.8	0.05	2.58
400	8.854	21.906	8.818	127.1	-2.9	130.0	0.02	2.02
500	8.862	22.040	8.817	83.1	-0.2	83.3	0.00	1.64
600	8.876	22.125	8.821	52.8	−0.3	53.2	0.01	1.30
800	8.896	22.234	8.822	31.2	−0.4	31.6	0.01	1.00
1000	8.926	22.292	8.832	14.0	−0.9	14.9	0.06	0.67
1200	8.960	22.313	8.845	5.6	−0.5	6.1	0.08	0.42
1500	8.992	22.330	8.845	2.8	0.6	2.2	−0.26	0.30
2000	9.013	22.331	8.810	3.3	1.5	1.8	−0.85	0.32

(1) the numerical diagrams (tables) showing the relative water content (volume) of various TS-classes described above. The content is expressed in percentage of the total volume of the sea, which is $\sim 5.4\times10^5\,\mathrm{km}^3$; hence one volumetric unit is $5400\,\mathrm{km}^3$ (Figures 3a, 3b). The dots in the diagrams correspond to the contents $< 0.01\%$;

(2) the diagrams for TS-classes showing heat content (enthalpy) in $10^{21}\,\mathrm{J}$ (Figures 4a, 4b), and salt content, in $10^{15}\,\mathrm{kg}$ (Figures 5a, 5b), for August and February, correspondingly. The dots in the diagrams show the heat content $< 0.01 \times 10^{21}\,\mathrm{J}$, and the salt content $< 0.01 \times 10^{15}\,\mathrm{kg}^2$ (The enthalpy was determined as $Q = c_p \rho T V$, where the specific heat capacity c_p and the density ρ were calculated as functions of temperature and salinity, and V is the volume of the prism. The rounding, say, of the enthalpy to the nearest $10^{21}\,\mathrm{J}$ is quite acceptable. Application of smaller units results in the emergence of overly large numbers, so that the estimates made with these numbers become superfluous and hence not sufficiently reliable.)

(3) the three-dimensional TSP-diagrams (P stands for the percentage content); one of them being constructed for the full salinity range, up to 22.6‰ for August (Figure 6). The February diagram is omitted because with the vertical scale adopted, the diagrams for August and February at $S > 20.6$‰ are very similar (implying the constancy of the deep-water content in summer and in winter); two other diagrams (Figures 7a, 7b) for August and February, respectively, are in the range of $S < 20.6$‰, with an enlarged vertical scale of percentage content. The two latter diagrams show distinctly the seasonal migration of near-surface waters manifested as the existence of a "ridge" corresponding to these waters in summer and its disappearance before February. This process was already described above qualitatively using TS-scatter diagrams as an example. The two latter diagrams complement this description very well. Some quantitative characteristics of this seasonal vertical migration will be given below.

Let us examine some results of the analysis of numerical TS-diagrams presented above. (Note that the left temperature scale in Figures 3 to 5 is inadvertently shifted downward by half a degree.) These diagrams for volume, enthalpy, and salt content are subdivided into four quadrants by the 8°C isotherm and the 20‰ isohaline. Three of the four correspond to the Black Sea waters, namely to the deep waters ($S > 20$‰), to the cold intermediate waters with $T < 8$°C (a traditional criterion), and to the surface waters. The subdivision of the Black Sea waters into three classes is consistent with the theory of TS-curves: this is the "mixing triangle" that fits into the generalized water mass diagram (see above). The lower right quadrant is empty: there

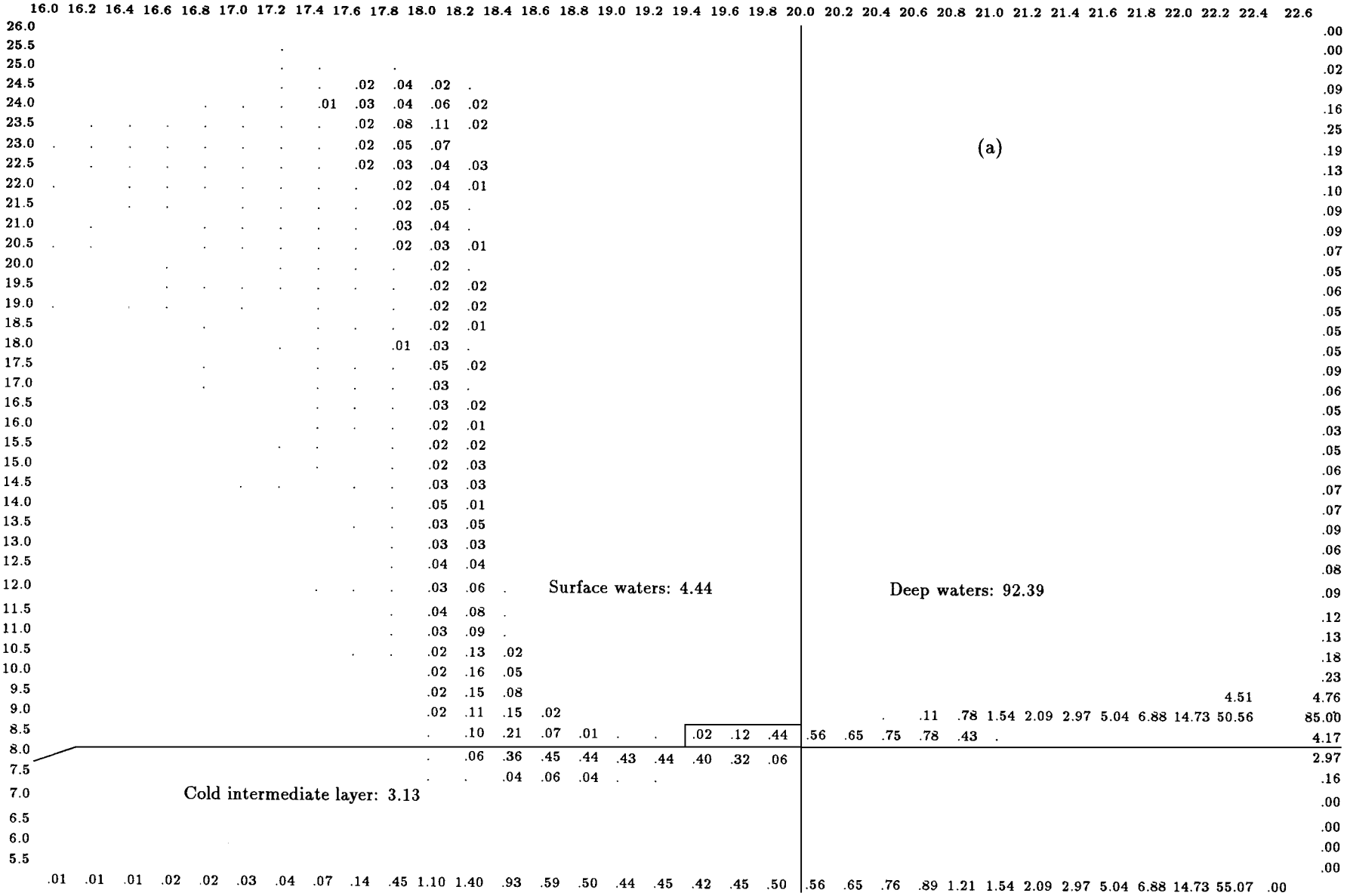

Figure 3. The volumetric TS-diagrams of the Black Sea waters by classes, in percentages of the total volume ($= 5.4 \times 10^5\,\mathrm{km}^3$). Points show the classes with the volumes $< 0.01\%$. Lower and right scales show the partial totals of percentages by columns and rows respectively. (a) August; (b) February. Left scale – Temperature, °C; Upper scale – Salinity, ‰.

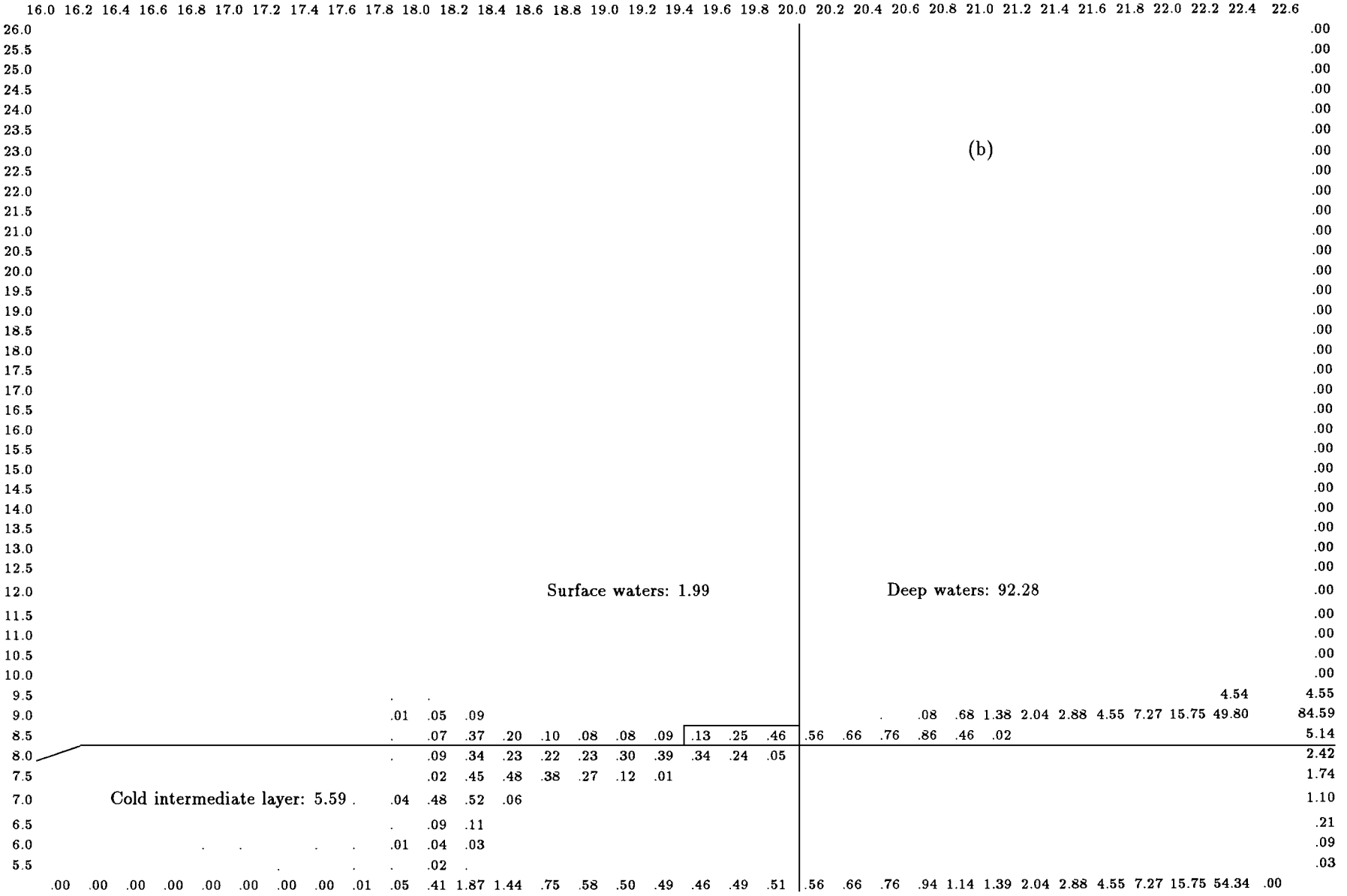

Figure 3. (continued).

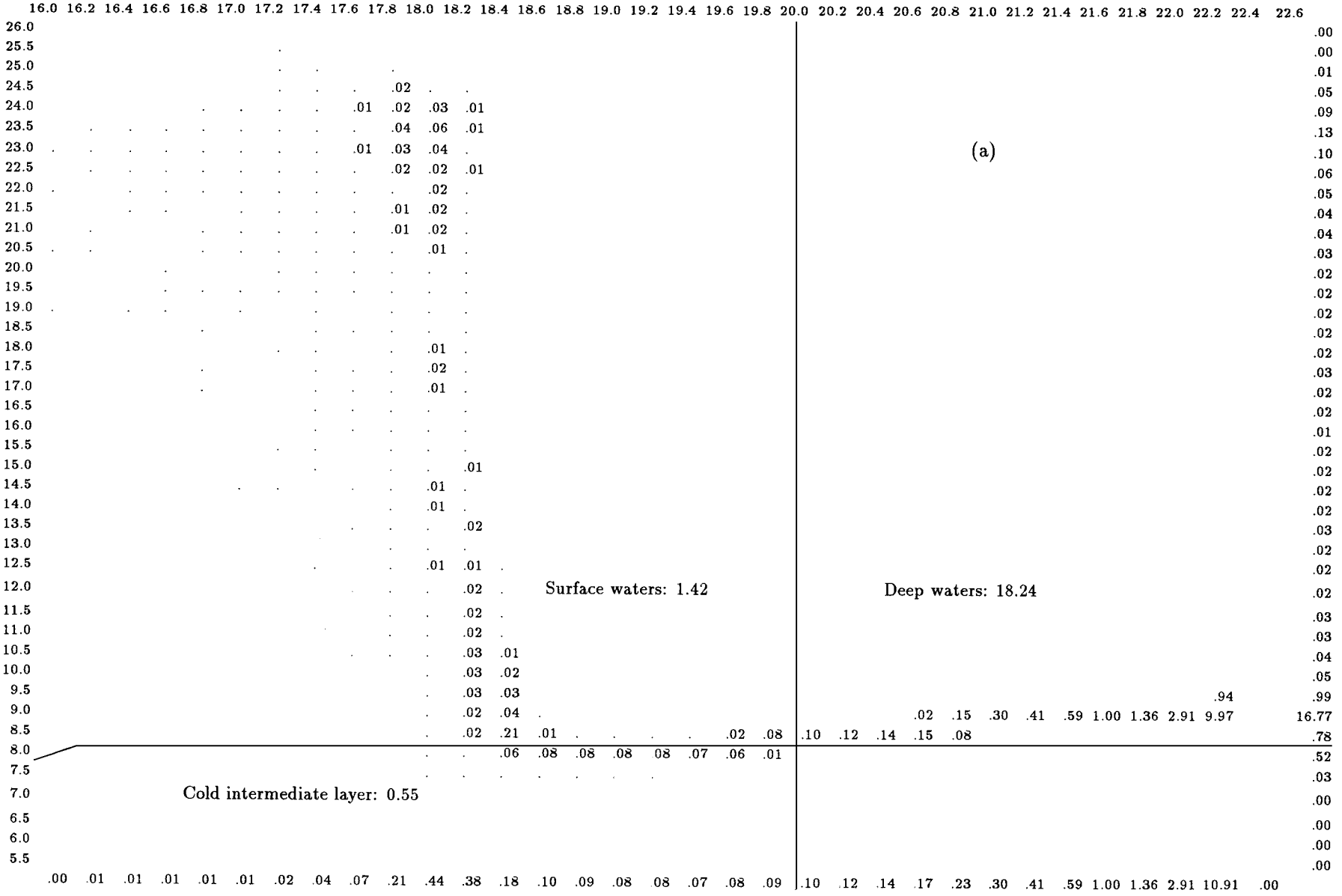

Figure 4. The TS-diagrams of enthalpy (heat content) of the Black Sea waters by classes, in 10^{21} J. Points show the classes with the heat content $< 0.01 \times 10^{21}$ J. (a) August; (b) February.

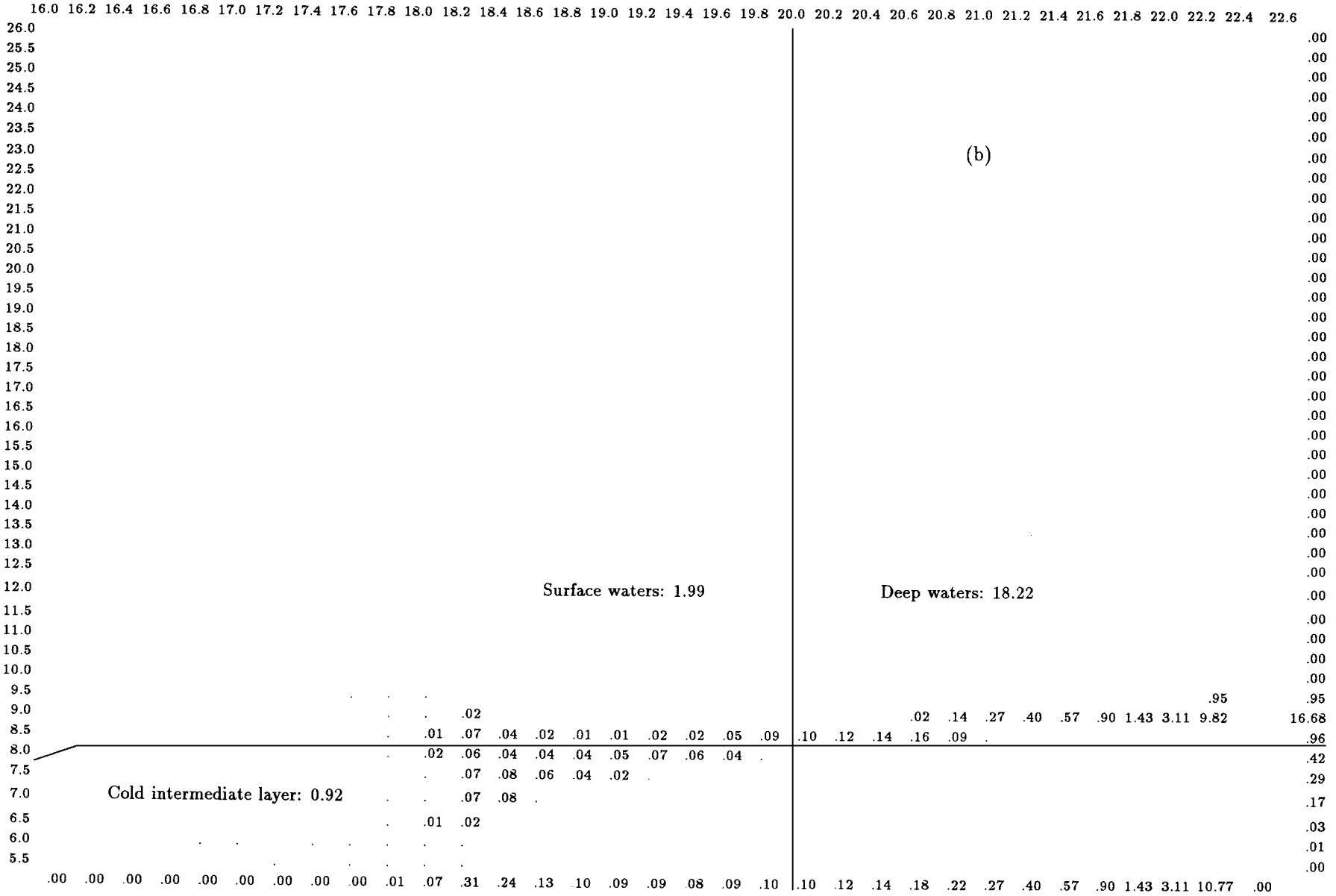

Figure 4. (continued).

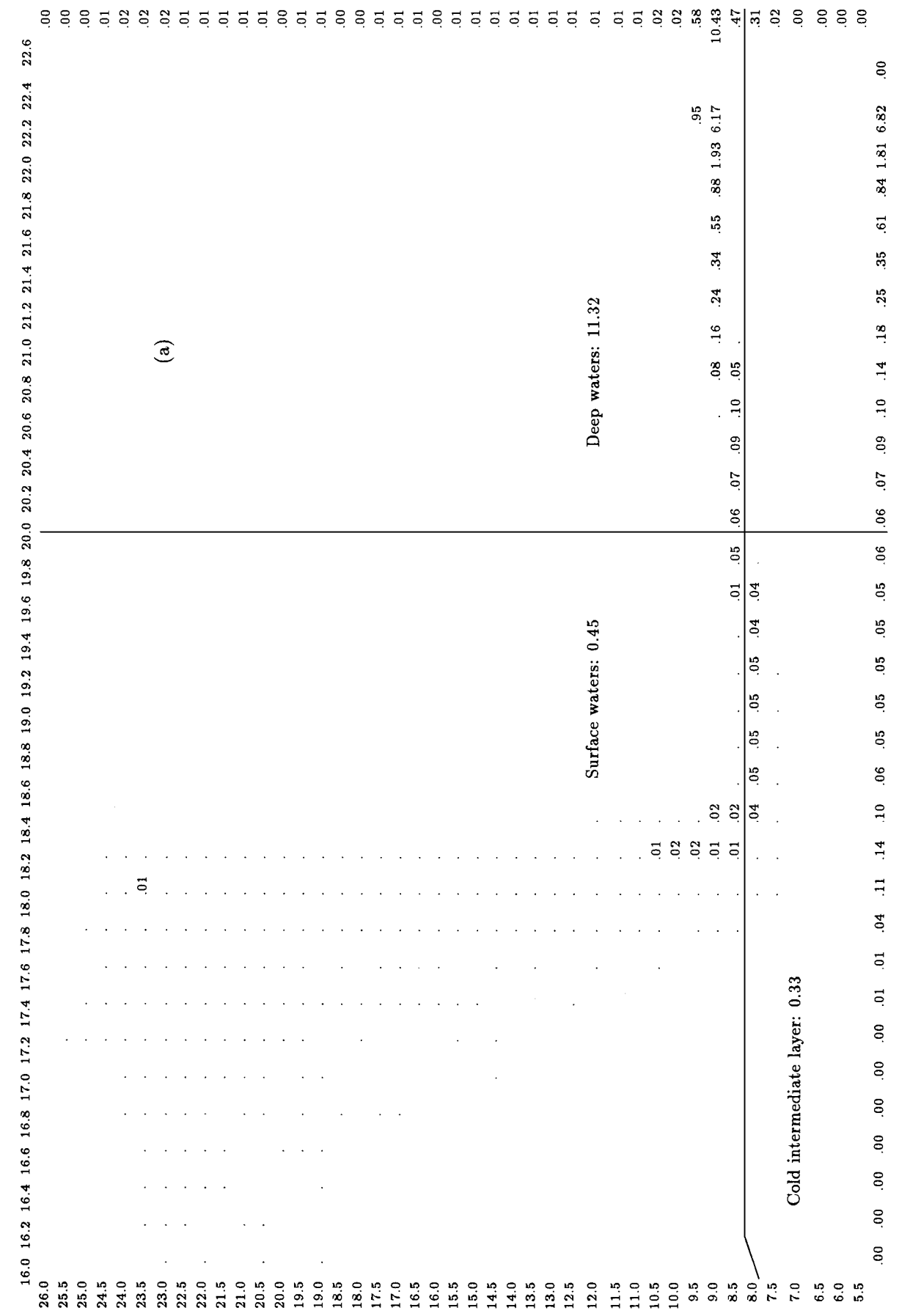

Figure 5. The TS-diagrams of salt content of the Black Sea waters by classes, in 10^{15} kg. Points show the classes with the heat content $< 0.01 \times 10^{15}$ kg. (a) August; (b) February.

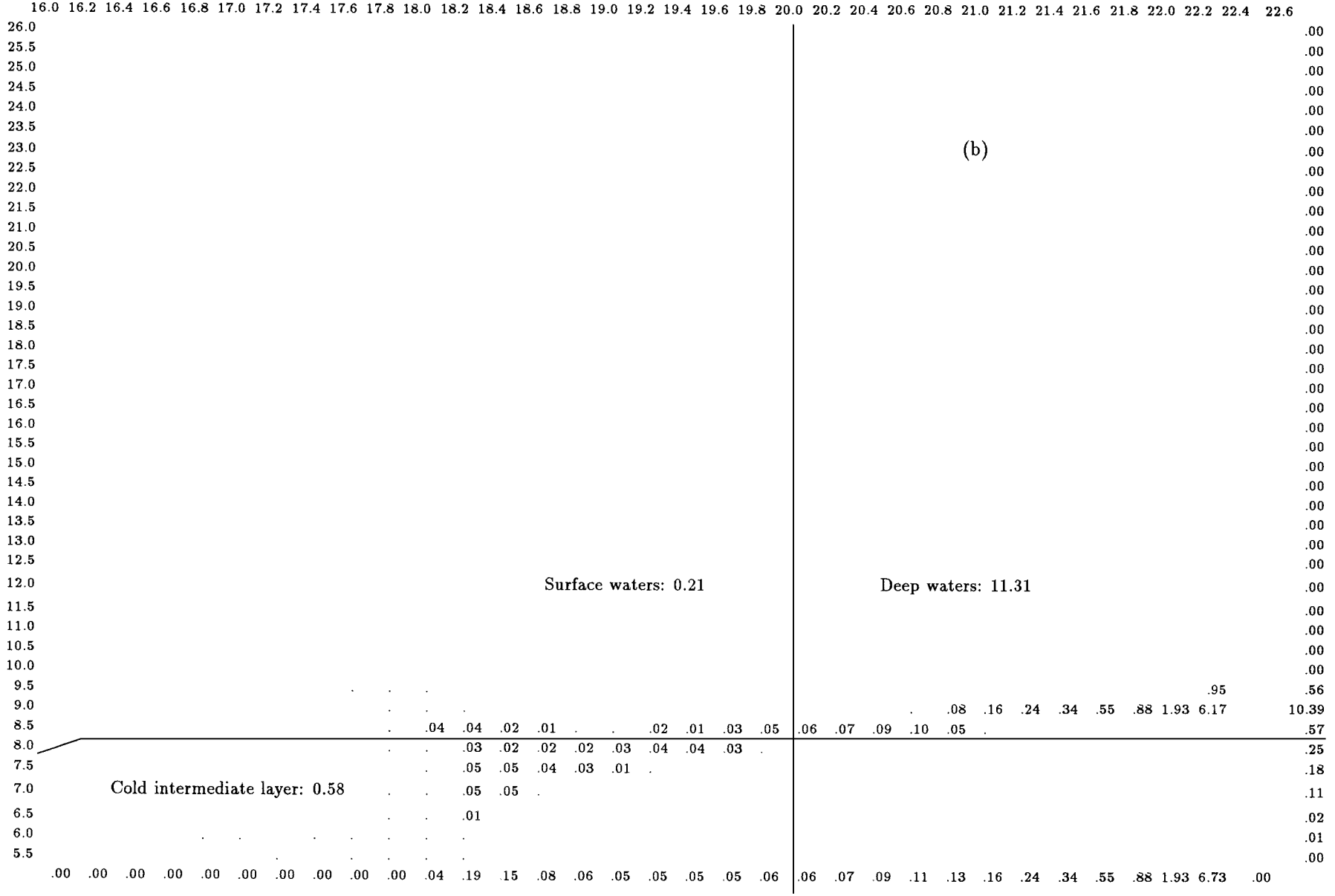

Figure 5. (continued).

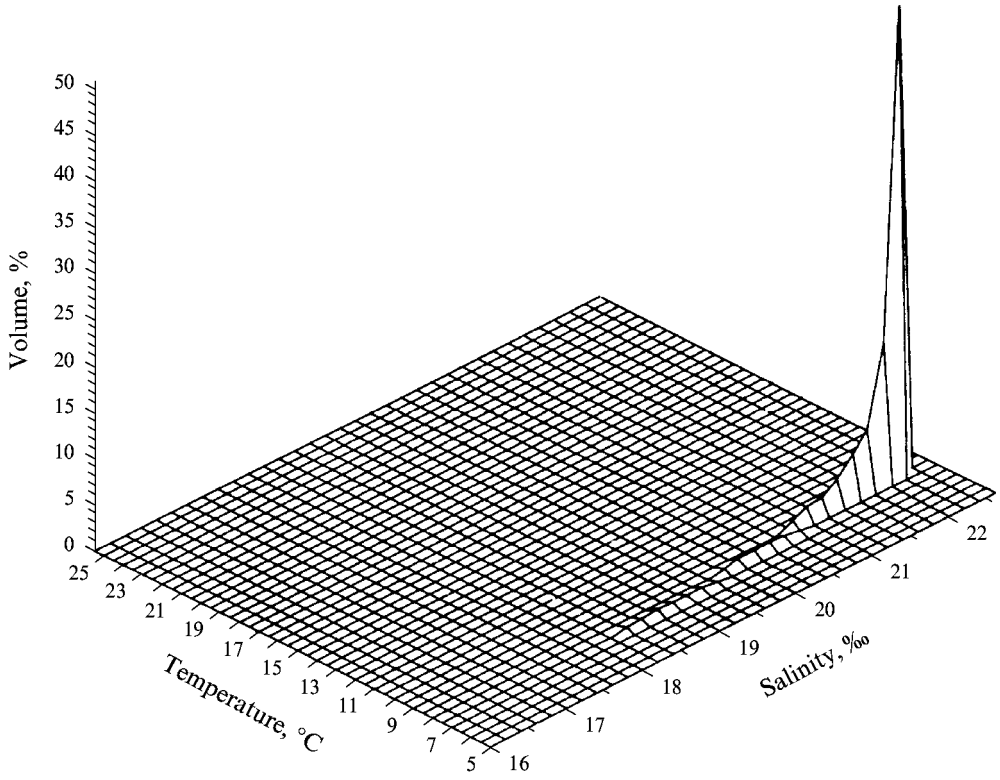

Figure 6. The three-dimensional TSP-diagram (P – percentage) of the Black Sea waters for August. A mountain peak ($\sim$ 51%) indicates the class with $8.5 < T < 9.0$°C, $22.2 < S < 22.4$‰.

are almost no waters with $S > 20$‰ at $T < 8$°C in the Black Sea. There is an uncertainty of the surface waters' definition, which is distinct when comparing the numerical diagrams with the scatter diagrams: with such a subdivision, the waters lying below the CIL (shown with the rectangle in the upper left quadrant of the volumetric diagrams in Figures 3a, 3b) fall into the surface water class. It seems likely that these waters, accordingly to Gertman's classification, are better classified as intermediate waters. However the same is true of the waters with $T < 8$°C (see the numbers under the rectangle and also the scatter diagrams), but this violates the convenient criteria of the CIL waters as the waters with $T < 8$°C, so that the overall picture would become unnecessarily complex. We leave this uncertainty, especially as it results in an insignificant error, not essential for subsequent reasoning. This error constitutes (by volume) 0.58% for August and 0.84% for February (taking into account the water with $T < 8$°C, we have to add another 0.78% for August and 0.63% for February). We assume (conditionally) that the CIL lies as though "within" the surface water's layer, and their common boundary lies somewhat deeper 100 m.

Using the numerical characteristics of the three main water masses shown in TS-diagrams, let us consider the seasonal variability of their volume and the heat/salt transfer between the layers.

Deep Waters

The deep waters ($S > 20$‰), as seen from the diagrams, constitute about 92% of the total volume of the Black Sea waters. The difference between August and February is so insignificant (it results rather from small errors of the volumetric diagram computation) that these waters could be regarded as isolated from the seasonal cycle. The deep waters are nearly homogeneous in temperature: 85% of the deep waters fall into a 0.5°C range ($8.5 < T < 9.0$°C). The salinity gradient, however, is significant, as could be seen from either volumetric diagrams, or the averaged TS-curve (Figure 8). This fact corroborates the Marmara Sea origin of the deep waters of the *Black Sea* [1991]. Just one TS-class ($8.5 < T < 9.0$°C, $22.2 < S < 22.4$‰) contains about 50% of the total water volume, illustrated by the "Mt Everest" of the deep water's topography: a peak in the three-dimensional TS-diagram (Figure 6).

The deep waters contain about 90% of the heat content and 94% of the salt content of the Black Sea.

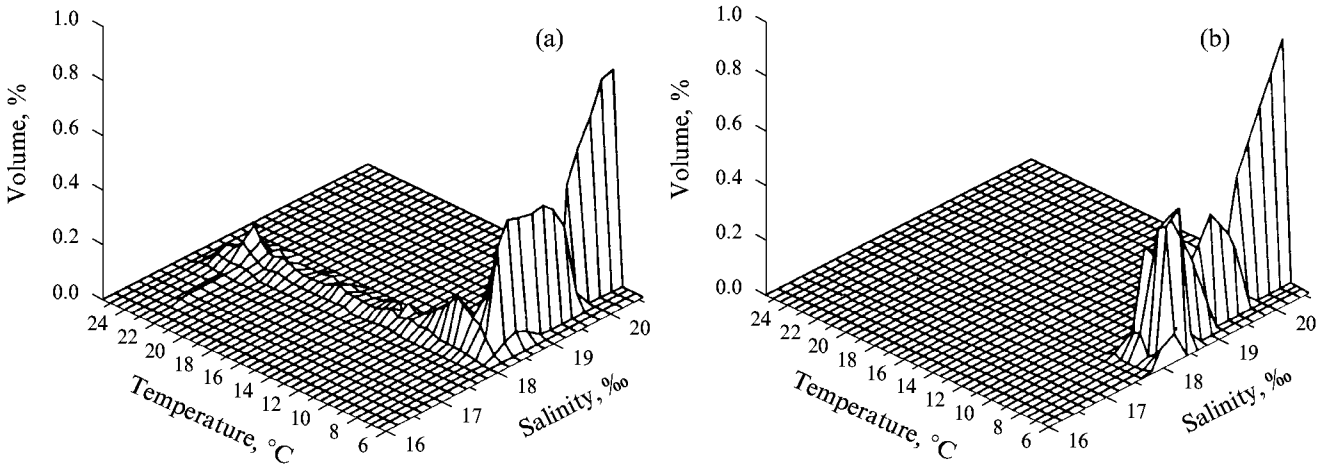

Figure 7. The three-dimensional TSP-diagrams of the Black Sea waters with the expanded percentage scale. (a) August; (b) February.

Surface Waters Plus Cold Intermediate Layer

The seasonal variability of integral characteristics of the thermohaline structure of the Black Sea waters encompasses these two layers, as shown above during the scatter diagrams' analysis; the volumetric diagrams allow us to augment this analysis quantitatively.

As was shown, in fall and winter the surface waters are cooled; the heat lost goes partially to the atmosphere, and partially to the CIL. The sum of the volumes of these two layers also remains constant. The "pumping" of volume, salt, and heat thus occurs from one layer into another, manifested as the transfer of corresponding numerical characteristics from one TS-quadrant into another.

The total volume of the surface waters plus the cold intermediate layer remains therefore unaltered: the surface water's "loss" is $4.44–1.99 = 2.45\%$; while the cold intermediate layer's "gain" is 2.46%, as seen from Figures 3a, 3b.

The evaluation of the salt transfer gives the same results, due to the conservation of the total salt content. From August through February, the surface water's loss of salt is $0.45–0.21 = 0.24\,(\times 10^{15}\,\mathrm{kg})$, while the corresponding CIL's salt gain is $0.58–0.33 = 0.25\,(\times 10^{15}\,\mathrm{kg})$.

Finally, let us examine the seasonal variability of the heat content. Between August and February, the surface layer's heat loss is $1.42–0.37 = 1.05\,(\times 10^{21}\,\mathrm{J})$, while the CIL's heat gain (from the surface layer) is $0.92–0.55 = 0.3\,(\times 10^{21}\,\mathrm{J})$; with the remaining $1.05–0.37 = 0.68\,(\times 10^{21}\,\mathrm{J})$ going to the atmosphere during the fall/winter cooling. Let us assume that this heat is given up from the entire surface of the sea, i.e., $423 \times 10^9\,\mathrm{m}^2$ [*Chernoye Morye*, 1991], so that from August through February (over six months), a unit area gives up $(0.68 \times 10^{21}\,\mathrm{J})/(423 \times 10^9\,\mathrm{m}^2) = 1.61 \times 10^9\,\mathrm{J\,m}^{-2}$, i.e., on average, $0.27 \times 10^9\,\mathrm{J\,m}^{-2} = 270\,\mathrm{MJ\,m}^{-2}$ per month. This estimate is comparable with published data, the monthly averaged maps of heat balance of the surface layer (Figure 1.10 on pp. 140–141 in *Chernoye Morye* [1991]). By these maps, the heat loss (in $\mathrm{MJ\,m}^{-2}$) in the "middle" point of the sea (halfway between Sarych Cape and Inebol Cape) is approximately 100 in September, 150 in October, 270 in November, 350 in December, 250 in January, and 50 in February, with the six-month average heat loss being $195\,\mathrm{MJ\,m}^{-2}$. Note that our estimate is the same as given in *Chernoye Morye* [1991] for November.

We omit a more detailed analysis of volumetric TS-characteristics. Note the overall agreement of our results with the data by Glazkov and Gertman. The only difference is that our estimates of the total salt and heat contents of the Black Sea are slightly higher than the estimates given by Gertman.

4. Average Oceanographic "Station"

This term will connote the averaged (over the entire area of the sea) temperature and salinity data for each standard level, for August and February. These data are shown in Tables 1 and 2, together with the following derivative quantities: potential temperature calculated by Bryden's polynomial [*Unesco*, 1993], vertical static stability E and its thermal (E_θ) and salinity (E_S) constituents, density ratio E_θ/E_S, and the Väisälä-Brunt frequency NB. The TS-curves of the average stations for August and February are shown in Figure 8 (cf. the scatter diagrams).

The average oceanographic station for August and February may be regarded as a "template" station, to be used to compute the thermal, salinity and other anomalies in various places of the sea, similar to the

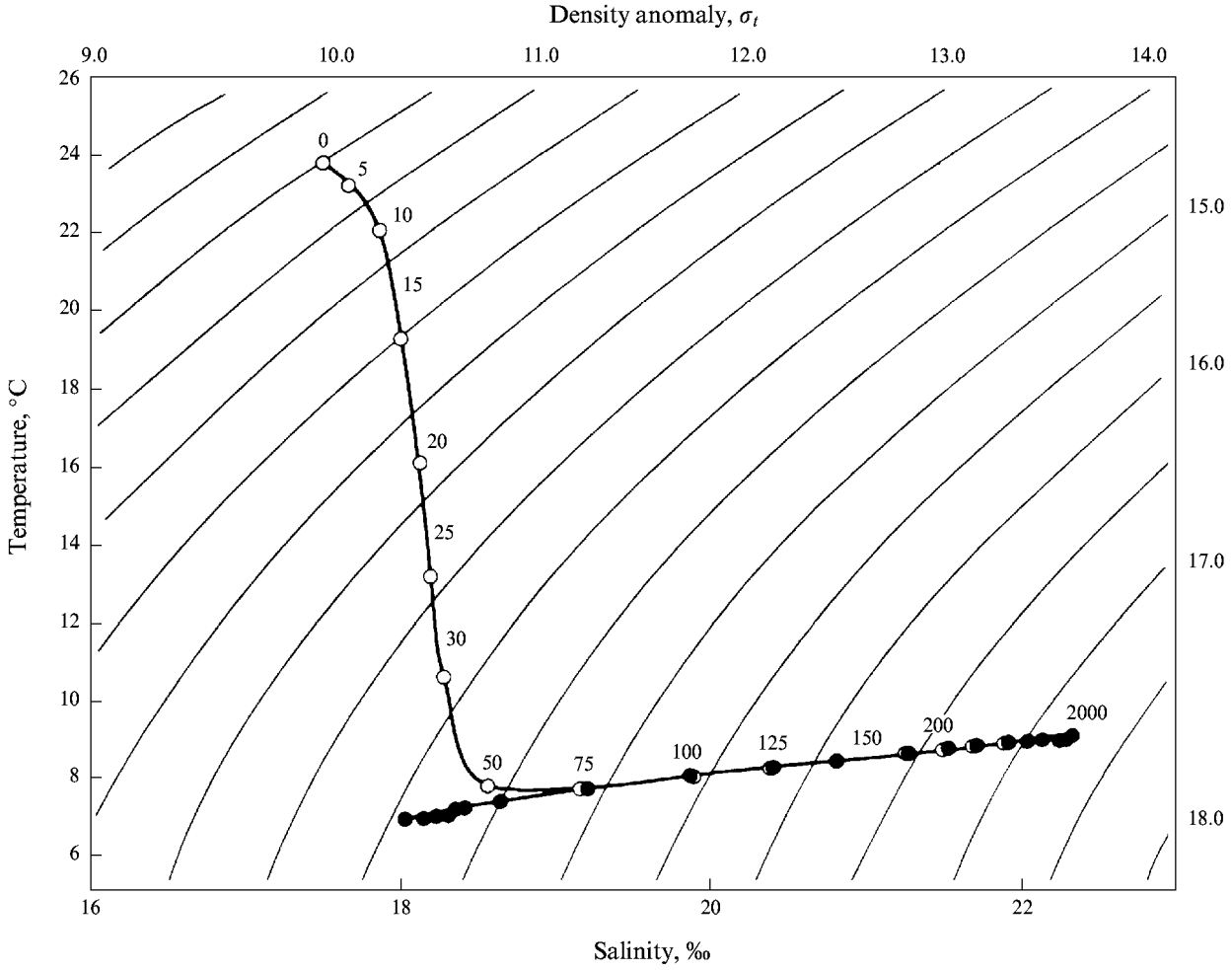

Figure 8. The average TS-curves of the Black Sea water masses for August (open circles) and February (solid circles). The numbers near the circles show pressure in dbar.

"salinity anomalies method" of Helland-Hansen and Nansen (see *Mamayev* [1987], Section 67), which is used to determine spatial differences and horizontal transformations, especially in the surface layer and in the CIL. We will not discuss this topic here and note only the following feature of the average data for August and February. In August, the pycnocline (the vertical stability maximum) and the thermocline (the E_θ maximum) are observed at ~ 15 m, beneath a thin upper layer of warm water, while the halocline is being observed at ~ 75 m. In February, the pycnocline and the halocline are observed at the same 75-m depth, the lower boundary of the cold intermediate layer. In winter, the thermal instability ($E_\theta < 0$) is observed across the entire water column, while in summer the instability it is observed only below 75 m (because above 75 mm significant thermal stability ($E_\theta < 0$) is observed). The salinity stability is positive across the entire water column year-around; it compensates for the thermal instability ($E_S > E_\theta$) everywhere except the 0–75 m layer in summer, so that the total stability is always positive, although it is small in deep layers. The frequencies of the thermohaline oscillations below 500 m vary between 0.3 and 1.7 cycle/hour.

5. Hydrological Database

This study was based on the database of hydrological observations made in the Black Sea in 1923–1991, mainly by Soviet ships. This database was compiled at the Department of Oceanography at the Moscow State University with the assistance of the Marine Hydrophysical Institute of the Academy of Sciences of Ukraine. The database included only those stations with both temperature and salinity measurements. The data were sorted by month, season, and half year. Geographically, the data were assigned to $21'$ latitude

by 28′ longitude cells, i.e., to squares 39 km × 39 km, so that the grid consists of 303 cells, with the origin at 41°N, 28°E. For each cell with data, the average temperature and salinity values were computed at each standard level, up to a maximum of 23 levels (0, 5, 10, 15, 20, 25, 30, 50, 75, 100, 125, 150, 200, 250, 300, 400, 500, 600, 800, 1000, 1200,1500, and 2000 m).

The August and February subsets consist of 8213 and 3663 stations, respectively. In August and February, the average values of temperature and salinity were calculated in 282 and 248 cells, comprising 93 and 83% of the Black Sea area, respectively. For other cells (without data), the temperature and salinity values were obtained by interpolation using the two-dimensional cubic beta-spline. The input data for the interpolation routine consisted of the long-term average values (and their standard deviations) from all the cells with data. In total, taking into account the scale of averaging, the estimates of mean values in adjacent cells in the upper 500-m layer differ statistically significantly with 95% probability. To assure the same reliability in the 500–1000 m layer, where the data volume is 5 to 6 times less than at the sea surface, the mean seasonal values were used for winter (January–March) and summer (July–September), while in the 1000–1500 m layer and below 1500 m the half yearly and annual averages were used, respectively.

References

Glazkov, V. V., Volumetric statistical T, S-analysis of the Black Sea water masses, *Oceanology, Engl. Transl., 10*, No. 6, 958–962, 1970.

Mamayev, O. I., Deep waters of the Black Sea, *Priroda, 12*, 70–78, 1986.

Mamayev, O. I., *Termokhalinnyy Analiza vod Mirovogo Okeana* (Thermohaline Analysis of the World Ocean Waters, 296 pp., Gidrometeoizdat, Leningrad, 1987.

Hydrometeorology and hydrochemistry of the seas of the USSR, in *Chernoye Morye, Gidropmeteorologicheskiye Usloviga* (The Black Sea, Hydrometeorogical Conditions, 429 pp., Vol. IV, Issue 1, Gidrometeoizdat, St. Petersburg, 1991.

Ozsoy, E., Z. Top, G. White, and J. M. Murray, Double diffusive intrusions, mixing and deep sea convection processes in the Black Sea, in *The Black Sea Oceanography*, edited by E. Izdar and J. M. Murray, pp. 17–42, NATO ASI Series, Kluver Academic Publishers, Dordrecht, 1991.

Fofonoff, N. P., and R. C. Millard, Jr., Algorithms for computation of fundamental properties of seawater, *UNESCO Tech. Pap. Mar. Sci. 44*, 53 pp., 1983.

(Received May 27, 1993.)